

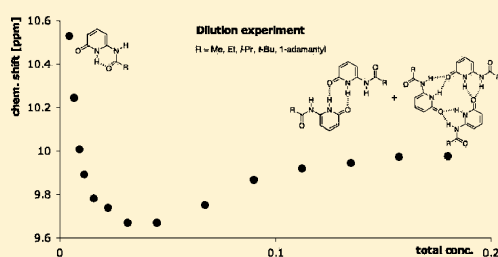
# 2-Acylamino-6-pyridones: Breaking of an Intramolecular Hydrogen Bond by Self-association and Complexation with Double and Triple Hydrogen Bonding Counterparts. Uncommon Steric Effect on Intermolecular Interactions

Borys Ośmiałowski,<sup>\*,†</sup> Erkki Kolehmainen,<sup>‡</sup> and Magdalena Kowalska<sup>†</sup>

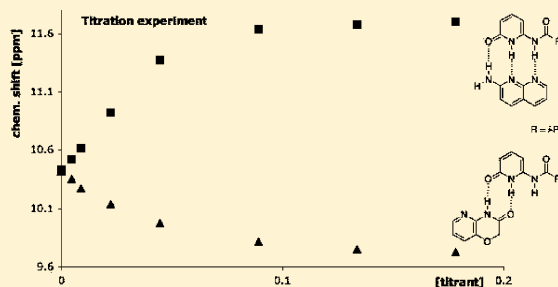
<sup>†</sup>Faculty of Chemical Technology and Engineering, University of Technology and Life Sciences, Seminaryjna 3, PL-85-326 Bydgoszcz, Poland

<sup>‡</sup>Department of Chemistry, University of Jyväskylä, P.O. Box 35, FI-40014 Finland

**S** Supporting Information



Self-association



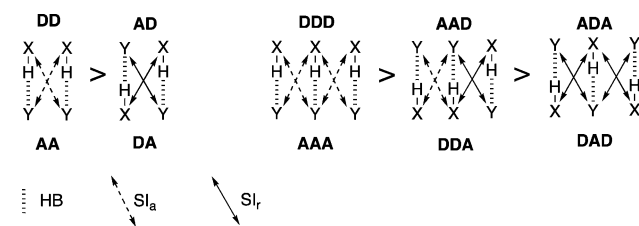
Heterocomplexation

**ABSTRACT:** 2-Acylamino-6-pyridones (acyl = RCO, where R = Me, Et, *i*-Pr, *t*-Bu, and 1-adamantyl) were previously characterized by X-ray diffractometry and solid-state NMR techniques by us. One of these compounds was used recently in organocatalysis. The series is now studied in solution and by computational methods recommended for noncovalent interactions (DFT/M05). These compounds showed interesting behavior during dilution and titration experiments monitored by <sup>1</sup>H NMR. 2-Acylamino-6-pyridones change their conformation at higher concentrations, forming double hydrogen-bonded dimers and trimers in which an uncommon steric effect is observed. To the best of our knowledge, this is the first example of such behavior of hydrogen-bonded molecules. Heterocomplexation of the studied compounds happens via double or triple hydrogen bonding, depending on the properties of the counterpart. The computation data support and explain the effects observed experimentally, including the tautomeric, closed/open form equilibrium and intermolecular interaction preferences.

## INTRODUCTION

Noncovalent interactions that are crucial in the formation of supramolecular assemblies depend on the shape and functional groups (including tautomeric preferences) of the interacting molecules. We have shown that tautomeric equilibria in some CH acids (2-phenaclypyridines and derivatives) and their intramolecular hydrogen bonding can be controlled by the character of the substituent, by benzoannulation<sup>1–5</sup> and by their molecular ability to maintain or lose their aromatic character.<sup>6</sup> The loss of aromatic character in one ring of substituted 1,8-naphthyridines allows these molecules to exist in a tautomeric form that self-associates by quadruple hydrogen-bonding. Our previously published papers on controlled homo- and hetero-association were focused on hydrogen-bonded heterocycles.<sup>7–12</sup> Secondary interactions (SIs, introduced by Pranata and Jorgensen<sup>13,14</sup>), which can be attractive (SI<sub>a</sub>) or repulsive (SI<sub>r</sub>), coexisting with hydrogen bonds in supramolecular assemblies, can influence their interaction energies.<sup>15–20</sup> The array of hydrogen bond donors (D) and acceptors (A) has influence on the type of their secondary interactions (Chart 1). For example, in quadruple

Chart 1. General Stability in Double and Triple Hydrogen-bonded Associates



hydrogen bonded assemblies, the DDDD/AAAA interacting motif is, in general, more stable than DADA/ADAD.<sup>21–24</sup> In addition, the acidity/basicity of hydrogen bond donors/acceptors influences the stability of the formed assemblies.

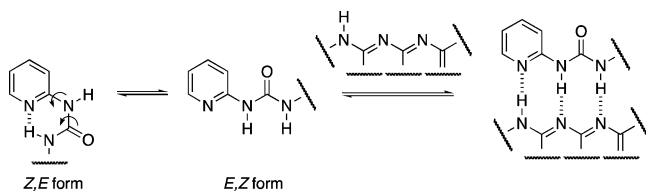
Further, strong intramolecular hydrogen bonding may result in fast proton exchange (tautomerism) between basic

Received: August 30, 2011

Published: January 17, 2012

centers.<sup>5,25</sup> If intramolecular hydrogen bonding occurs resulting in a closed conformation, then breaking of this bond is a crucial step before any heteroassociation might happen.<sup>26</sup> There are examples of urea derivatives<sup>27</sup> that crystallize as closed (*Z,E* isomer) or open (*E,Z* isomer) form, depending on the substituent position in *N*-methylated pyridine. On the other hand, the 2-pyridylurea derivatives that are not salts crystallize in a *Z,E* (closed) form.<sup>26,28,29</sup> The same compounds can interact with hydrogen bonding counterparts giving heteroassociates with an *E,Z* conformation (Chart 2).<sup>26,27,30–32</sup>

Chart 2. Example for Association of 2-Pyridylurea



The classical 2-pyridone/2-hydroxypyridine tautomeric pair is the simplest example of heterocyclic compounds that can form dimers.<sup>16,33–35</sup> In fact, it is claimed to be the most stable double hydrogen bonded dimer known.<sup>36</sup> However, SIs can influence the stabilization of corresponding dimers yielding even higher interaction energies.<sup>12</sup> Regarding hydrogen bonding, 2-pyridone is comparable to 2-acylaminopyridine but their difference arises from the possibility of controlling the self-association of the latter molecules by the steric effect of the substituent.<sup>8</sup> We have recently studied the steric and electronic effect on the association in triple and quadruple hydrogen-bonded complexes.<sup>7,9–11</sup> The steric effect is also responsible for the hydrogen bonding to ester oxygen (C=O) in the solid state of dihydropyridinone derivative, while in pyridone derivative hydrogen bond is bifurcated (C=O...H(N)...O=C-OR).<sup>37</sup> In the current study, an inspiring idea was to combine the topologies of 2-pyridone and 2-acylaminopyridine and to study how the steric effects influence the intra- and intermolecular interactions in 2-acylamino-6-pyridones (Chart 3).

It is worth pointing out that open forms of 2-acylamino-6-pyridones (N form)/2-acylamino-6-hydroxypyridines (O form) can self-associate, giving dimers (or higher aggregates) with different energies of stabilization owing to different SIs<sup>13,14</sup> (Chart 4). The same chart shows other compounds used in the current study.

Chart 3. Superposition of Topologies of 2-Pyridone/2-Hydroxypyridine and 2-Acylaminopyridine and Possible Forms of Resulting Structures

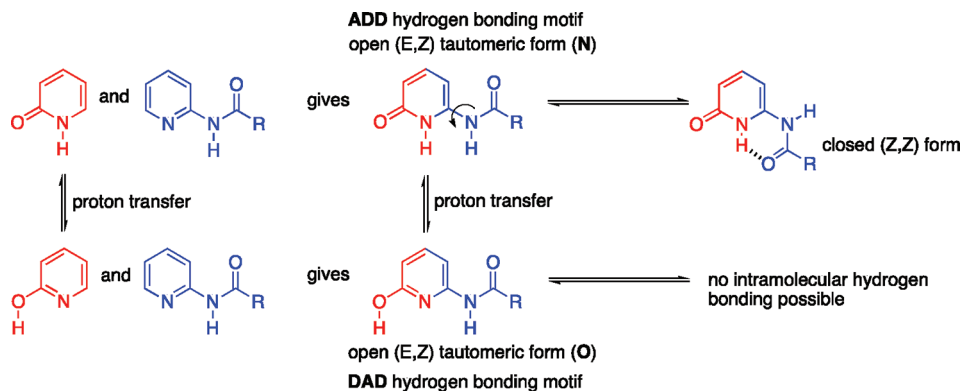
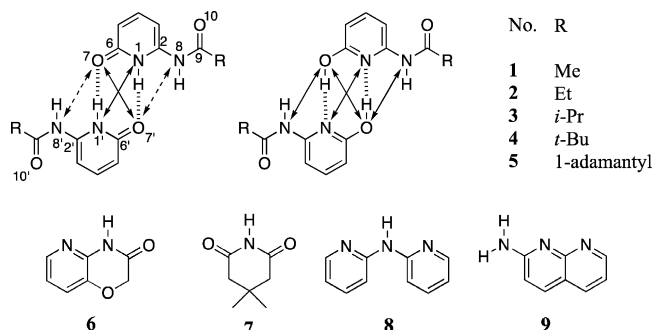


Chart 4. Dimers of 2-Acylamino-6-pyridones/2-Acylamino-6-hydroxypyridines with Secondary Interactions, Atom Numbering and Hydrogen-bonding Counterparts

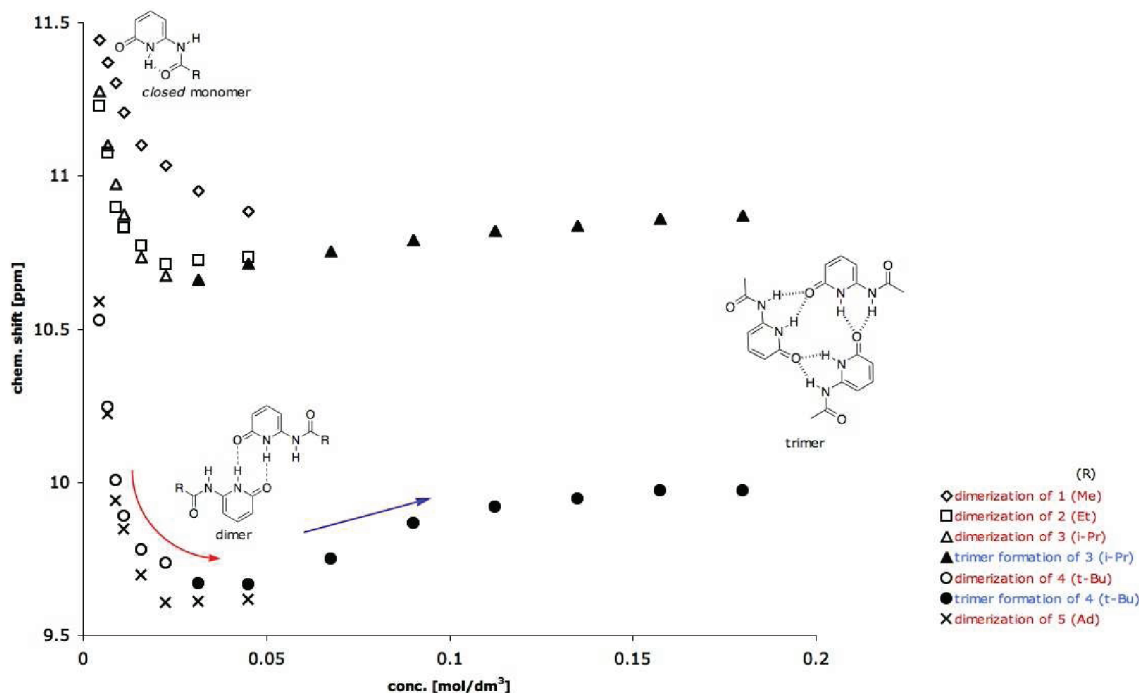


Since these compounds are used in organocatalysis,<sup>38</sup> an understanding of their intermolecular interactions is crucial. The detailed aims of this work are to clarify (a) the tautomeric preferences of 2-acylamino-6-pyridones, (b) the steric effect on self-association, (c) the type of heterocomplexation with counterparts capable of double and triple hydrogen bonding, and (d) whether 2-acylamino-6-pyridone can be converted into 2-acylamino-6-hydroxypyridine upon complexation by a preceding 1,3-proton shift (tautomeric equilibrium).<sup>39</sup> The studied compounds exist in the solid state as closed (*Z,Z*) pyridone form,<sup>40</sup> and the hydrogen bonding pattern of open pyridone form (N) is similar to that of guanine.

## RESULTS AND DISCUSSION

The first step in studying the intermolecular interactions in 2-acylamino-6-pyridones was a series of dilution experiments. The behavior of  $\delta(\text{H1})$  as a function of concentration is shown in Chart 5.

It is known that generally the [monomer]/[dimer] ratio decreases as a function of increasing total concentration. This is observed as a monotonous change (increase) in the proton chemical shifts involved in hydrogen bonding. In this case the behavior of the proton chemical shifts is more complex. At very low concentrations, the  $\delta(\text{H1})$  is high and decreases until the concentration reaches ca. 0.045 mol/dm<sup>3</sup>; then  $\delta(\text{H1})$  starts to increase. This behavior suggests that at low concentrations the intramolecular hydrogen bond stabilizes the closed form and that a H1...O10 hydrogen bond is preferred if there is a lack of a potent hydrogen bonding counterpart (low concentration). The dilution data indicate that equilibrium exists between

Chart 5.  $\delta(\text{H1})$  as a Function of Concentration in Anhydrous  $\text{CDCl}_3$ 

closed monomer, dimer of the open form and, trimer of the open form. Due to existence of intramolecular hydrogen bond it is reasonable to say that the concentration of the open monomer is much smaller than that of the closed monomer form. For compounds **3** and **4** the dilution data were divided into two sets (Chart S1, Supporting Information). For remaining compounds only first part of the dilution curves were used for calculation of dimerization constants ( $K_{\text{dim}}$ , Table 1).

Table 1.  $K_{\text{dim}}$  and  $K_{\text{tri}}$  Values [ $\text{M}^{-1}$ ] Based on  $\delta(\text{H1})$  Changes

compound	$K_{\text{dim}} \times 10^2$	$K_{\text{tri}}^a \times 10^2$
1	4.0	
2	6.0	
3	8.0	2.2
4	8.0	2.5
5	9.0	

<sup>a</sup>The dimer + monomer  $\rightleftharpoons$  trimer reaction is assumed (see also Chart 11).

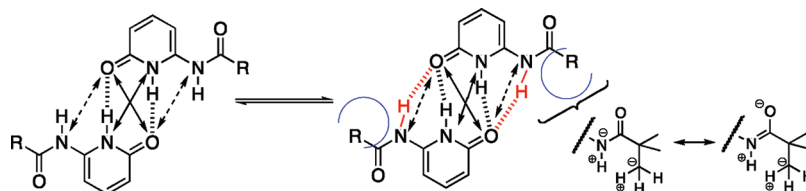
The first point (the highest chemical shift of H1) was removed from calculations. We have assumed that at this point the chemical shift refer to the presence of purely closed (*Z,Z*, Chart 3) form in  $\text{CDCl}_3$  solution. Even a visual inspection of the dilution curves show that the changes of  $\delta(\text{H1})$  upon concentration increase are higher in **5** than in **1**, for example. The trimerization constants ( $K_{\text{tri}}$ ) are listed only for two congeners due to the limited solubility of remaining ones. The additional chart (Chart S2, Supporting Information) representing the absolute changes in  $\delta(\text{H1})$  vs. total concentration ( $|\Delta\delta(\text{H1})|$  vs.  $[\text{conc.}]$ ) shows normalized dilution curves. These show clearly more dramatic changes in H1 chemical shift for compounds with larger substituents.

In our previous studies the more bulky substituent caused weaker associations<sup>8–10</sup> but here this phenomenon is reversed. This uncommon steric effect can be explained by the steric interaction between substituent R (Chart 6, in blue) and H8. This effect might be supported by weak dipole–dipole

interaction of NH and CH bonds. Thus the larger substituent pushes the H8 proton more effectively toward the O7' of another molecule in the pyridone homocomplex. Combined with that an attractive SI turns into a weak hydrogen bond (Chart 6, in red). These hypotheses are further verified by calculations at M05 level and with the use of the dispersion corrected (for chosen monomers only, SI) functional (later in text). The values of  $K_{\text{tri}}$  for compounds **3** and **4** are comparable to that of other double hydrogen bonded complexes. According to Sartorius and Schneider<sup>41</sup> the self-association of cytosine is expressed by  $K_{\text{dim}}$  equal to  $40 \text{ M}^{-1}$ , while for 2-acylaminopyridines carrying various substituents in the acyl group it is less than  $20 \text{ M}^{-1}$ .<sup>8,42</sup> The dimer of cytosine is stabilized by two  $\text{NH}\cdots\text{N}$  hydrogen bonds and an  $\text{NH}/\text{O}$  attractive secondary interaction, while the repulsion in 2-acylaminopyridines is caused by the size of the substituent. The molecules of guanine have a hydrogen-bonding pattern similar to the molecules studied here. The self-association constant for guanine is 290 or  $300 \text{ M}^{-1}$  depending on the proton used as a probe (the same order as  $K_{\text{dim/tri}}$  found for **1–5**).<sup>41</sup> The difference between the dimerization of cytosine (with two attractive SIs) and that of guanine most probably comes from the fact that in guanine the attractive SIs turn into weak hydrogen bonds of  $\text{NH}\cdots\text{O}$  type (as in Chart 6) or higher aggregates are formed. Other homo/heterocomplexes held together by double hydrogen bonding have  $K_{\text{dim/assoc}}$  of the order of  $10^2\text{--}10^3 \text{ M}^{-1}$ .<sup>32,43–45</sup>

The methine CH proton in **3** is used as a probe<sup>11</sup> for studying association as well. At higher concentrations only one septet was observed, while at low concentrations there were two (spectra in Supporting Information). The molar ratio of the two forms is expressed by function  $[\text{associate}]/[\text{monomer}] = 2.8442 \ln[3] + 16.607$  with  $R^2 = 0.9965$ , where the  $[\text{associate}]/[\text{monomer}]$  ratio was calculated by integration of the respective signals. At the lowest concentration ( $0.00445 \text{ mol/dm}^3$ ) the difference between the chemical shifts of observed methine protons was 0.32 ppm.

Chart 6. Bulkiness of the Substituent as a Driving Force for Dimer Stabilization



To test further the behavior of the studied compounds, VT (variable temperature)  $^1\text{H}$  NMR spectra were recorded for **1** (compound with the smallest R). The  $^1\text{H}$  and  $^{13}\text{C}$  NMR spectra in  $\text{CDCl}_3$  were recorded at +30, +10, -10, -30, -40, -50, and -60  $^\circ\text{C}$  for  $^1\text{H}$  NMR spectra and +30  $^\circ\text{C}$  and -30  $^\circ\text{C}$  for  $^{13}\text{C}$  NMR spectra (Supporting Information) at the same concentration. The results show significant differences in the spectra suggesting that at higher temperatures the open hydrogen-bonded associate is present, while at lower temperatures the closed monomer coexists with the complex. The deshielding of H1 due to hydrogen bonding shows that the multiple intermolecular  $\text{NH}\cdots\text{O}$  interactions are able to compete with the intramolecular hydrogen bonding. Table 2

Table 2.  $^1\text{H}$  NMR Chemical Shifts [ppm] for **1** in  $\text{CDCl}_3$  as a Function of Temperature

temperature [ $^\circ\text{C}$ ]	H1 (associate) <sup>a</sup>	H1 (closed monomer)	H8 (closed monomer)
-60	13.49	11.98	9.05
-50	13.24	11.84	8.84
-40	13.16	11.76	8.65
-30	13.10	11.66	8.46
-10		11.49	~8.20 <sup>b</sup>
10		11.30	8.02
30		11.05	7.91

<sup>a</sup>H8 signal in the associated molecules is not observed. <sup>b</sup>Overlap with aromatic protons.

shows the H1 and H8 chemical shifts for **1** recorded at various temperatures. The integration data were used to assign H1 and H8 signals to the respective forms. The observed chemical shifts are in agreement with the GIAO<sup>46,47</sup> calculated values (see Supporting Information for chart and comment).

Together with the shifting of the respective NH peaks, the signals of aromatic protons (H3 and H5) sharpen when the temperature is raised (spectra in Supporting Information). This suggests that a fast exchange in the NMR time scale takes place at high temperature—a rotation around the C2–N8 and N8–C9 bonds.

The  $^1\text{H}$  NMR titration further tested the ability of 2-acylamino-6-pyridones for intermolecular interactions preceded by breaking of the intramolecular hydrogen bond. The heterocomplexation in the studied compounds can happen in two ways, that is, forming triple and double hydrogen-bonded

complexes (Chart 7). However, the latter demands a proton transfer yielding 2-acylamino-6-hydroxypyridines that form a heterocomplex with the ADA counterpart.

The compounds used in this study offer both hydrogen-bonding patterns. To avoid precipitation during titration, only compounds **3** and **4** were used in the experiments. Due to the fact that compounds **7** and **8** are similar (both symmetric and having an ADA hydrogen bonding pattern), the former was excluded from the titration of **3**. Charts 8 and 9 show the titration curves of **3** and **4** with the use of H1 as a probe.

A comparison of the data presented in Charts 8 and 9 shows that due to steric reasons the heteroassociation of **3** and **4** with the same counterpart is different. However, there are also similarities. First of all, both compounds associate by triple hydrogen bonding with **9** although *t*-Bu derivative associate effectively after reaching a [titrant]/[titrated compound] ratio of ca. 2 (increasing  $\delta(\text{H1})$ ). Degradation of the trimeric form is most probably responsible for the decreasing part of the curve in heterocomplexation of **4** with **9**. For both **3** and **4**, titrant **6** acts as a factor that breaks the intramolecular hydrogen bond in the closed monomer and decomposes the self-associated aggregates. Finally, there is a difference between binding **8** with **3** and **4**. Compound **3** carrying an *i*-Pr group associates more effectively with **8** (Chart 8, inset), while the larger *t*-Bu group in **4** hinders this. As was mentioned before, the methine CH proton may also be used as a probe-nucleus in measuring the association of hydrogen-bonded molecules.<sup>11</sup> Chart 10 shows the change of methine CH chemical shift of **3** during titration. On the basis of these data, the  $K_{\text{assoc}}$  (on chart) were calculated.

The association of **3** with **9** is stronger than with other titrants (triple vs. double hydrogen bonded complex) but it is worth noting that the values obtained from non-hydrogen-bonded atoms may be only approximate. However, the  $K_{\text{assoc}}$  of  $110\text{ M}^{-1}$  found with the use of  $\delta(\text{H1})$  in titration of **3** with **9** (Chart 8) is in agreement with the data presented in Chart 10. While in Chart 8 the curve of **3**+**6** titration shows a monotonous decrease in chemical shift, the methine CH shows clearly that these molecules associate. The same is realized in titrations of **4** by **6**–**8** but cannot be confirmed directly by monitoring of CH chemical shift. Anyhow, the decrease of NH chemical shift during dilutions and titration is related to the close-to-open configurational change driven by intermolecular hydrogen bonding. This, in turn, suggests that when the total concentration during dilution is increased the increase in NH

Chart 7. Possible Triple and Double Hydrogen-bonded Associates of 2-Acylamino-6-pyridones

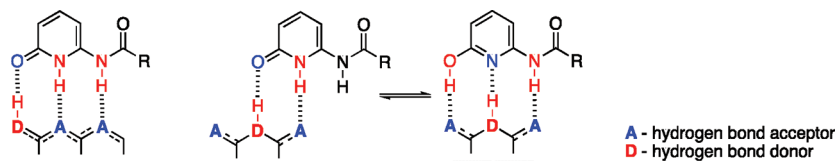


Chart 8. Titration Curves for 3

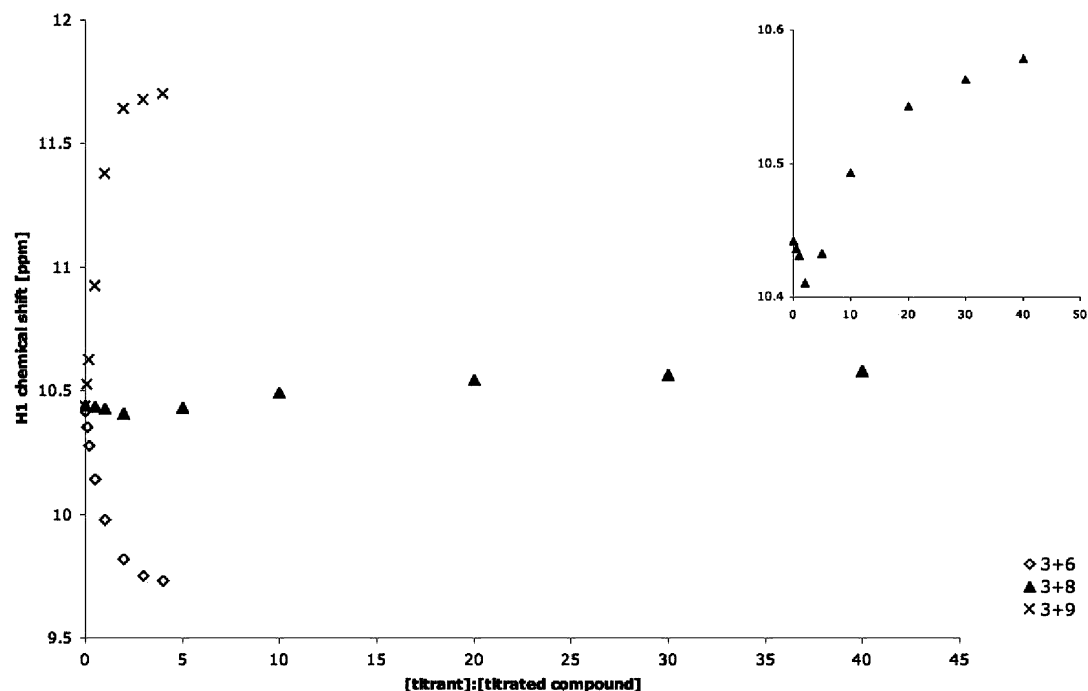
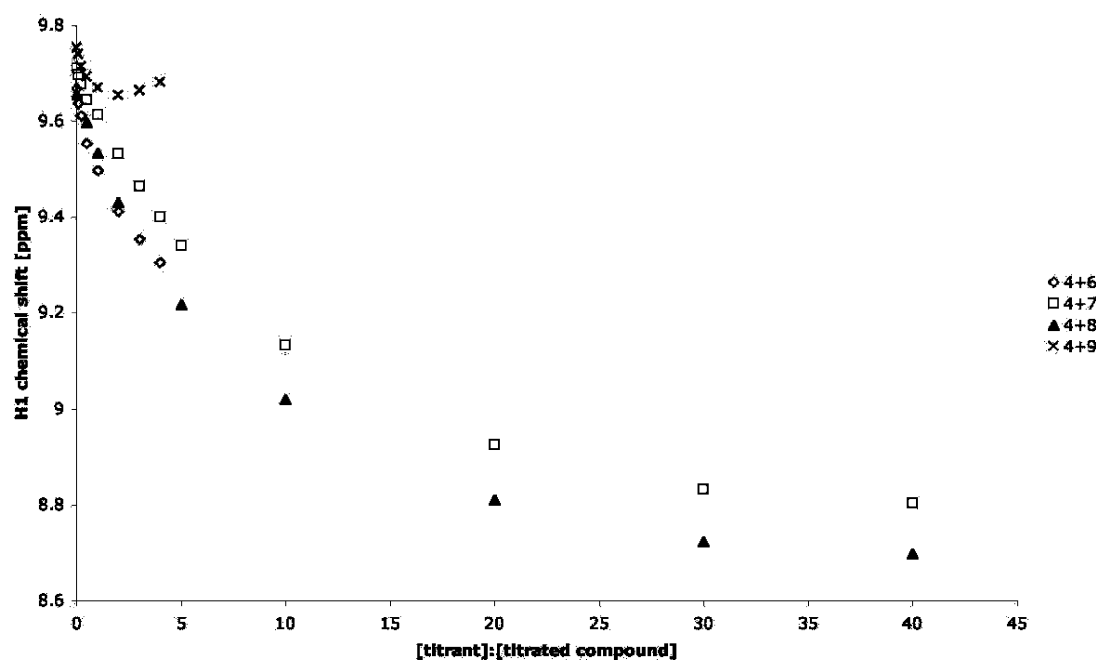


Chart 9. Titration Curves for 4



chemical shift is caused by the presence of higher aggregates (trimers). Moreover, any change of the chemical shift upon increased concentration of interacting molecules is related to the different ratios of respective forms. One curve is responsible for two different forms. Since the dilution data for 3 and 4 may be divided into two curves, at least three different species are present in solution (closed monomer and the dimer and trimer of the open form).

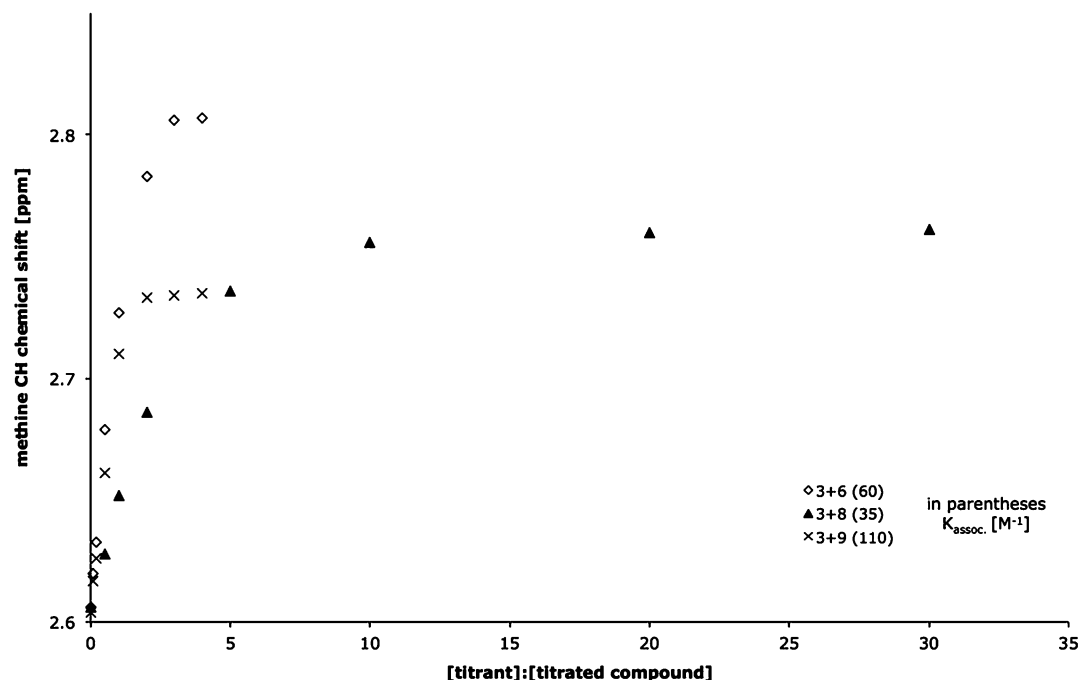
The computations at the DFT level including optimizations of monomers, dimers, heterocomplexes and transition states in proton transfer reaction in subjected compounds shed additional light on the properties of these molecules. Table 3

collects the geometrical data for optimized 2-acylamino-6-pyridone dimers.

A comparison of hydrogen bond distances in dimers of two tautomeric forms (the geometry data of the dimers of 2-acylamino-6-hydroxypyridines are collected in Table S1, Supporting Information) shows that these distances are almost constant for  $Y-H\cdots X$  and  $Y-H\cdots X$  in both tautomeric forms. It is interesting that the  $O7-O7'$  distances in pyridone dimers (N) become larger when the size of the substituent increases, while  $N1-N1'$  behave in a reversed manner. This may be due to additional stabilization of the dimer by weak  $O7'\cdots H8$  hydrogen bonding or by  $O7'/H8N8$   $SI_a$ . Extra stabilization of



Chart 10. Methine CH Chemical Shifts during Titration

Table 3. Selected Structural Parameters: Distances [Å] and Angles [deg] for Pyridone Dimers<sup>a</sup> Optimized at the M05/6-311+G(d,p) Level with PCM Model of Solvation

	1	2	3	4	5
H1...O7'	1.792	1.791	1.791	1.802	1.806
N1-O7'	2.817	2.816	2.816	2.823	2.826
N1-N1'	3.552	3.551	3.548	3.504	3.507
O7-O7'	3.679	3.679	3.681	3.733	3.735
O7'...H8	2.416	2.415	2.411	2.328	2.331
O7-N8	3.291	3.291	3.287	3.224	3.227
C6-C6'	4.157	4.158	4.156	4.167	4.170
C2N8H <sub>8</sub>	115.5	115.5	115.5	114.8	114.9
N1H1O7'	173.2	173.1	173.1	171.2	171.1
N8H8O7'	144.4	144.4	144.5	147.1	147.1
N1N8O7'	57.3	57.3	57.3	58.7	58.7
N1C2N8	113.3	113.5	113.3	113.1	113.1
C2N8C9	127.9	128.0	128.0	128.1	128.2
N8C9Ca(R)	114.0	112.9	114.0	114.2	114.3

<sup>a</sup>Primed atoms belong to another molecule in the dimer.

dimers by large substituents can be explained by van der Waals interaction of the substituent R with the proton H8 forcing it toward O7' in the dimer (Chart 6). It is also possible that dipole-dipole repulsion between N8-H8 and C-H bonds of the substituent contributes to the overall interactions.

The influence of the size of R on intermolecular distances is visible in the O7'...H8 distance and the N8H8O7', C2N8C9, N1C2N8 and C2N8H8 angles (see also the geometry optimized with the use of the dispersion corrected functional in Supporting Information). It is important to mention that both heterocyclic rings occupy a common plane.

Table 4 collects the calculated interaction energies between the molecules in pyridone ( $E_{\text{int(N)}}$ ) and hydroxypyridine ( $E_{\text{int(O)}}$ ) dimers as well as the energy needed for monomer Z,Z to E,Z isomerization (breaking the H1...O10 hydrogen bond).

Table 4. Interaction Energy of Dimers ( $E_{\text{int(N)}}$  and  $E_{\text{int(O)}}$ ) [kJ/mol]

form	1	2	3	4	5
$E_{\text{int(N)}}$	-73.2	-73.6	-74.1	-74.4	-75.8
$E_{\text{int(O)}}$	-44.1	-44.4	-44.0	-43.8	-46.9
Closed-to-open energy <sup>a</sup>	14.2	14.2	13.0	12.1	14.8

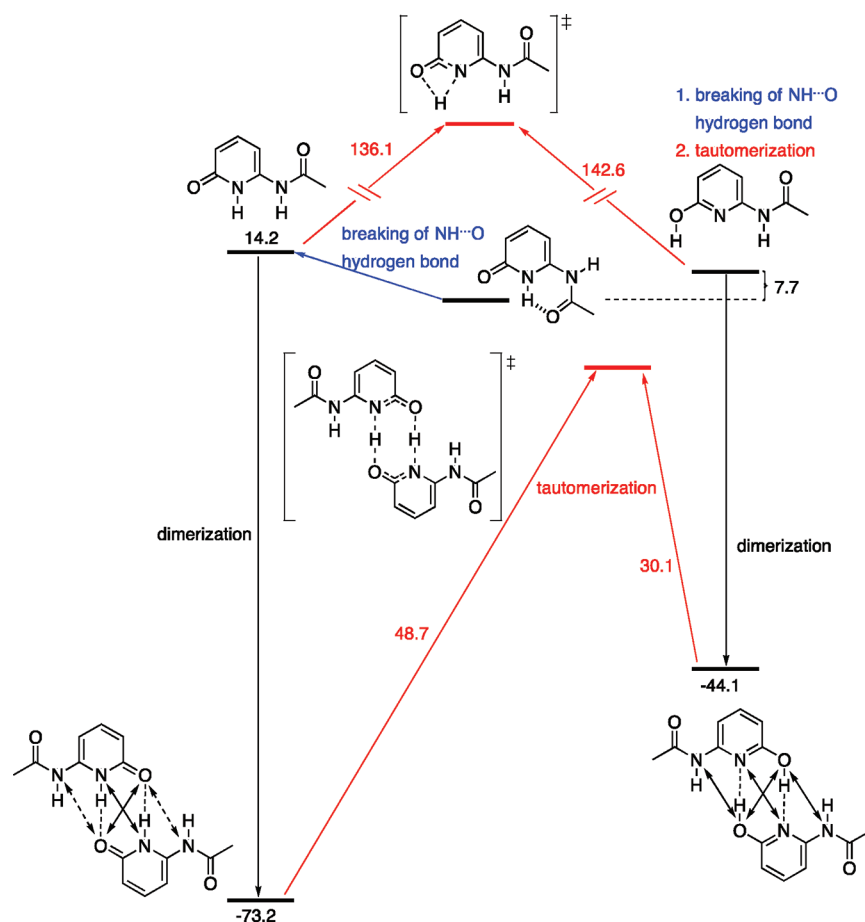
<sup>a</sup>Closed-to-open energy is the energy needed by the closed pyridone form to change the N1C2N8C9 dihedral angle from 0° to 180° (Z,Z → E,Z change, Chart 3).

The energy data show that the dimer with the highest interaction energy is 5. Merely these numbers (together with the geometry parameters) show that steric hindrance might affect the dimer stabilization. Scheme 1 shows the relations between the energies of monomers, dimers and transition states in 1.

The activation energy of the proton transfer within the monomer or the dimer shows that the calculations are in agreement with the experiment for this relatively complicated equilibrium.

The optimized geometry of dimers was used to calculate the H-BCP (Hydrogen Bond Critical Point) properties with the use of QTAIM<sup>48</sup> methodology. This methodology states that for covalent bonds the Laplacian ( $\nabla^2\rho$ ) of the electron density is negative while it is positive for noncovalent ones, such as closed-shell hydrogen bonds.<sup>48,49</sup> Recently we have used QTAIM together with the Espinosa<sup>50,51</sup> approach to study the intra- and intermolecular hydrogen bonding.<sup>12,52</sup> Here the same method was used to test how hydrogen bonding changes with the increasing size of the substituent. Table 5 collects the  $\nabla^2\rho$  (Laplacian of electron density),  $\rho$  (electron density) for H-BCPs and  $E_{\text{HB}}$  (hydrogen bond energy) data.

It is interesting to note that the QTAIM derived values for hydroxypyridine dimers (in italics, Table 5) are practically constant. On the other hand, in pyridone dimers the larger substituent influences the hydrogen bonding, that is, the Laplacian, density and hydrogen bond energy increase for the H8...O7' interaction and decrease for H1...O7'. This is a proof that the

Scheme 1. Energy [kJ/mol] Diagram for **1** (PCM, Chloroform)<sup>a</sup>

<sup>a</sup>The dashed and solid arrows represent attractive and repulsive secondary interactions, respectively.

bulky substituent pushes the N(8)–H(8) bond toward oxygen O7', yielding a shift of molecules (Chart 6), strengthening H8...O7' and weakening H1...O7' hydrogen bond. While the relative numbers obtained by the Espinosa approach do not differ much from each other, they still support the observed intermolecular interactions in dimers. Moreover, the difference between the sum of hydrogen bond energies (−95.8 kJ/mol for **1**) and  $E_{\text{int}}$  (Table 6) is very close to the sum of  $\text{SI}_r$  energy<sup>53</sup> (27.6 kJ/mol). This shows that  $E_{\text{int}}$  is close to the sum of the individual interactions.

In optimized dimers, the sterically interacting moieties are rotated in such a way as to obtain the weakest interaction with H8, that is, in **4** the dihedrals of O10–C9–C(R)–C(H<sub>3</sub>) are 0, 120 and 240° (rotamer A, Scheme 2). The rotation about the C9–R bond causes the CH<sub>3</sub> to be much closer to H8 and therefore increase the steric hindrance (said O10–C9–C(R)–C(H<sub>3</sub>) would then be 180, 60 and 300°, rotamer B, Scheme 2).

The data in Table 5 show that in the closed form the intramolecular hydrogen bond becomes stronger as the substituent gets larger. This is in agreement with the X-ray determined geometry.<sup>40</sup>

Since dimer formation alone did not explain the chemical shift behavior upon dilution, calculations also taking trimer into account were included. Due to the large computational cost, other higher associates were not considered, which also can be justified by entropy reasons. Chart 11 shows the formation of two different trimers used in the calculations.

Table 5.  $\nabla^2\rho$  and  $\rho$  at H-BCP and the  $E_{\text{HB}}$  [kJ/mol] in Pyridone and Hydroxypyridine (italics) Dimers and in the Closed Pyridone Form (bold)

R	$\nabla^2\rho$ , $\rho$ , $E_{\text{HB}}$ H1...O7', H7...N1', H1...O10	$\nabla^2\rho$ , $\rho$ , $E_{\text{HB}}$ H8...O7'
1	0.120, 0.037, −40.71	0.033, 0.008, −7.18
2	0.121, 0.037, −40.83	0.033, 0.008, −7.19
3	0.120, 0.037, −40.85	0.034, 0.008, −7.26
4	0.118, 0.037, −39.72	0.040, 0.010, −8.59
5	0.117, 0.036, −39.31	0.040, 0.010, −8.54
1	0.098, 0.039, −41.34	<i>a</i>
2	0.098, 0.039, −41.60	<i>a</i>
3	0.099, 0.039, −41.96	<i>a</i>
4	0.098, 0.039, −41.36	<i>a</i>
5	0.097, 0.039, −41.25	<i>a</i>
1	<b>0.105, 0.027, −27.40</b>	
2	<b>0.104, 0.027, −27.40</b>	
3	<b>0.105, 0.027, −27.93</b>	
4	<b>0.108, 0.028, −28.71</b>	
5	<b>0.107, 0.028, −28.45</b>	

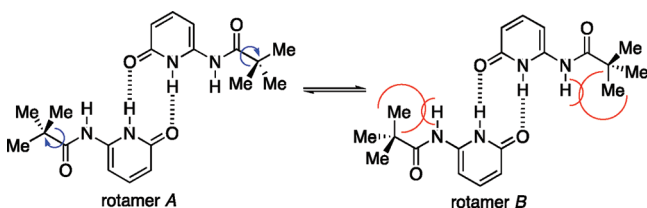
<sup>a</sup>H-BCP not found.

The most important feature in trimeric structures is the bifurcated hydrogen bonds similarly as in dimers (Charts 4 and 6). The reaction from a dimer to a trimer can happen by breaking two hydrogen bonds (perturbed dimer, Chart 11). An insertion of an open monomer forming a complementary hydrogen-bonding pattern with a perturbed dimer yields a flat trimer, which was

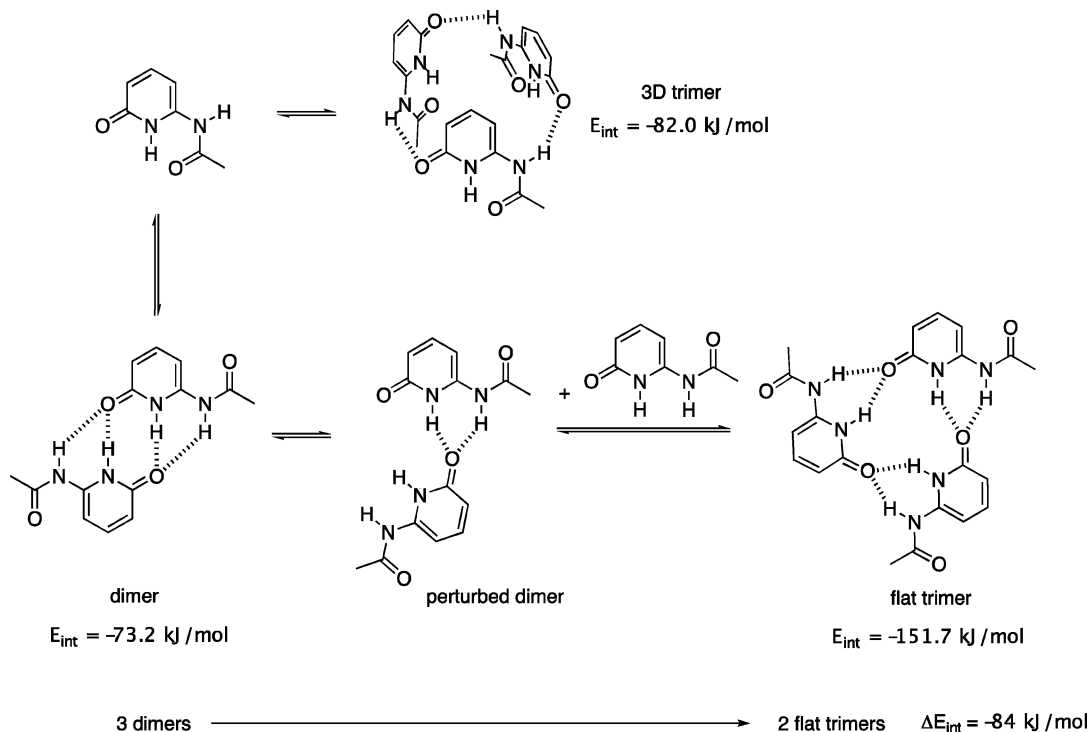
**Table 6.** Energy of Interactions [kJ/mol] of **1** with Various Counterparts

counterpart	triple hydrogen-bonded complex	double hydrogen-bonded complex
6	−48.0 (a), −41.5 (b) <sup>a</sup>	−43.5 (a), −35.7(b) <sup>a</sup>
7	−42.8	−41.2
8	−49.5	−31.4
9	−66.4	−34.7

<sup>a</sup>Two forms (a and b) are possible (pyridone form + **6** complexes are shown in Scheme 2. Triple hydrogen bonded associates of 2-hydroxy-6-acylamino pyridines are presented in Supporting Information).

**Scheme 2.** Influence of *t*-Bu Group Rotation on Push-effect on H8

energetically optimized. The same was done for the other 3D trimer. Trimer formation is in agreement with Etter's rules<sup>54</sup> which states that a good hydrogen bond donor interacts with a good hydrogen bond acceptor. It is easy to see that the reaction shown in Chart 11 is exothermic and the molecules of **1** tend to maximize the number of favorable (attractive) interactions and minimize the number of unfavorable (repulsive) ones. There are no SIs present in flat trimer due to the bifurcated character of hydrogen bonds. The reaction  $3 \times \mathbf{1}_2 \rightarrow 2 \times \mathbf{1}_3$  creates an increase of energy of interaction ( $\Delta E_{\text{int}}$ , Chart 11) by 84 kJ/mol. In both dimers and trimers the sum of the  $E_{\text{HB}}$  is close to the  $E_{\text{int}}$ . The QTAIM derived data (Supporting Information) for trimers support that.

**Chart 11.** Reaction Yielding **1**<sub>3</sub> from **1**<sub>2</sub>

The computations made for monomers and heterocomplexes allowed us to calculate the energy of interaction between subject molecules composing triple and double hydrogen bonded aggregates. Table 6 shows the energy of interaction between the studied compounds in various tautomeric forms that are capable of different types of association.

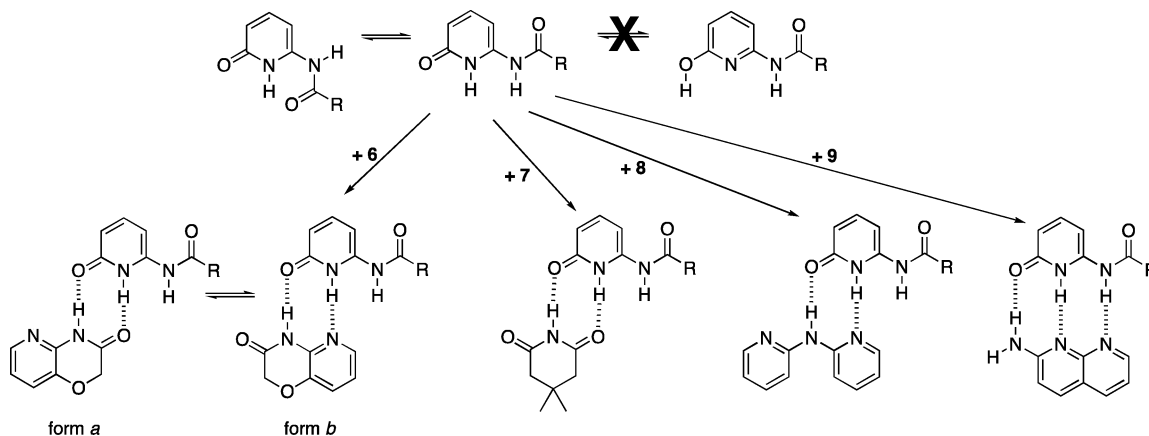
The difference in the energy of interaction between triply and doubly hydrogen-bonded complexes is smaller than, or close to, the *Z,Z*-to-*E,Z* isomerization energy (Table 4). This isomerization is the first step in the formation of hydrogen-bonded complexes. Even a double hydrogen-bonded interaction of subject molecules is able to break the intramolecular hydrogen bond. The highest interaction energy in the series is reported for **1** + **9** complex. These results are in agreement with the data obtained in titration experiments (Chart 8 and 9) and show that due to their relatively high activation energy (Scheme 1 and ref 12), no hydroxy form is present in heterocomplexes with ADA hydrogen bonding counterpart. The studied complexes are instead stabilized by two hydrogen bonds. Scheme 3 shows the heterocomplexes that are present in the studied mixtures.

## CONCLUSIONS

Five 2-acylamino-6-pyridones with varying sizes of acyl moieties exist in a closed conformation in the solid state. These compounds have been studied in solution by NMR spectroscopy and modeled with DFT methods. The dilution experiments revealed interesting results, indicating that the studied molecules exist in a closed (*Z,Z*) conformation, but when the concentration is increased, the dimerized/trimerized open (*E,Z*) form prevails. The stability of these associates is a reverse of the general steric crowding. This is caused by the pushing of the NH proton by bulky substituent toward the oxygen atom of the counterpart within the homocomplex. The heterocomplexation experiments showed that the pyridone form is the only one present in a chloroform solution and this



Scheme 3. Heterocomplexes of 2-Acylamino-6-pyridones



form is able to associate via double or triple hydrogen bonding, depending on the counterpart. The calculations (geometry optimizations, interaction energy, properties of the hydrogen bond critical point) support the experimental findings.

## EXPERIMENTAL SECTION

The synthesis of studied compounds is described in detail elsewhere.<sup>40</sup> Their purity and structure was confirmed by melting point measurements, elemental analysis, <sup>1</sup>H, <sup>13</sup>C and <sup>15</sup>N NMR spectra both in solution and in solid state. The liquid state <sup>1</sup>H and <sup>13</sup>C NMR and 2D PFG <sup>1</sup>H, <sup>1</sup>H COSY, PFG <sup>1</sup>H, <sup>13</sup>C HMQC and PFG <sup>1</sup>H, X (X = <sup>13</sup>C and <sup>15</sup>N) HMBC spectra were recorded with NMR spectrometer equipped with an inverse detection probehead and a z-gradient accessory for structure verification and chemical shift assignments. For three compounds the crystal structure was solved by X-ray diffractometry.<sup>40</sup> Titrants, that is, 2H-pyrido-[3,2-b]-1,4-oxazin-3(4H)-one (6), 4,4-dimethylpiperidine-2,6-dione (7), and dipyrindin-2-ylamine (8), used in this study were commercially available except 2-aminonaphthyridine (9). This compound was synthesized as described earlier.<sup>55</sup> The spectroscopic characterization for 9 is available in Supporting Information.

The dilution and titration studies were performed in anhydrous CDCl<sub>3</sub> purchased from Aldrich. δ(H1) was used as a probe in <sup>1</sup>H NMR dilution and titration experiments. Self-association constants ( $K_{\text{dim/tri}}$ ) were calculated according to reported procedures.<sup>56</sup> The Benesi-Hildebrandt equation<sup>57</sup> was used to calculate association constants ( $K_{\text{assoc}}$ ). The starting concentration of 1–5 in dilution studies and titrations were 0.00445 and 0.0445 mol/dm<sup>3</sup> (constant concentration), respectively. The concentrations during titration experiments were set to a value close to the minimum value of δ(H1) observed during dilution experiments (see text and explanation in Supporting Information). Unfortunately only two compounds (3 and 4) were soluble enough to give the full data set in dilution experiments. On the other hand the remaining three compounds behave in a similar way in the available concentration range. The titration was continued until the next portion of solid aliquots did not change the H1 chemical shift more than 0.1 ppm from that obtained in the previous step, or until precipitation occurred.

The calculations were carried out with Gaussian03<sup>58</sup> software at the M05/6-311+G(d,p)<sup>59–64</sup> level suggested for noncovalent interactions.<sup>60,61</sup> The PCM<sup>65</sup> model of solvation was applied (chloroform). For all monomers, dimers, trimers and heterocomplexes frequency calculations were performed to ascertain that the geometry corresponds to the energy minimum (only positive frequencies were obtained). The interaction energy between hydrogen-bonded associates was obtained as the difference between the energy of a dimer/trimer (corrected to the BSSE, Basis Set Superposition Error, correction by the counterpoise method<sup>66,67</sup>) and the sum of energies of two/three monomers. To shorten the article, only pyridone (the more stable form) geometries are discussed in the main text. The

remaining geometries are collected in Supporting Information. The transition states of the proton transfer reaction in monomers and dimers were found with the use of the Synchronous Transit-Guided Quasi-Newton<sup>68</sup> algorithm. The energies shown in Scheme 1 are ZPE (Zero-Point Energy) corrected. The calculations related to QTAIM (Quantum Theory of Atoms in Molecules)<sup>48</sup> methodology were performed with the use of AIM2000<sup>69</sup> software.

## ASSOCIATED CONTENT

### Supporting Information

<sup>1</sup>H, <sup>13</sup>C NMR spectra, detailed NMR data, chosen various temperatures and concentration spectra, dilution data charts/curves, pictures, Cartesians and energies of the optimized structures. This material is available free of charge via the Internet at <http://pubs.acs.org>.

## AUTHOR INFORMATION

### Corresponding Author

\*borys.osmialowski@utp.edu.pl

### Notes

The authors declare no competing financial interest.

## ACKNOWLEDGMENTS

Financial support from the Polish Ministry of Science and Higher Education (grant no. N N204 174138) is gratefully acknowledged. We are very much indebted to the ICM in Warsaw for providing computer time and programs.

## REFERENCES

- (1) Kolehmainen, E.; Osmialowski, B.; Krygowski, T. M.; Kauppinen, R.; Nissinen, M.; Gawinecki, R. *J. Chem. Soc., Perkin Trans. 2* **2000**, 1259–1266.
- (2) Kolehmainen, E.; Osmialowski, B.; Nissinen, M.; Kauppinen, R.; Gawinecki, R. *J. Chem. Soc., Perkin Trans. 2* **2000**, 2185–2191.
- (3) Gawinecki, R.; Kolehmainen, E.; Loghmani-Khouzani, H.; Osmialowski, B.; Lovasz, T.; Rosa, P. *Eur. J. Org. Chem.* **2006**, 2006, 2817–2824.
- (4) Osmialowski, B.; Kolehmainen, E.; Nissinen, M.; Krygowski, T. M.; Gawinecki, R. *J. Org. Chem.* **2002**, 67, 3339–3345.
- (5) Osmialowski, B.; Kolehmainen, E.; Gawinecki, R. *Chem.—Eur. J.* **2003**, 9, 2710–2716.
- (6) Raczynska, E. D.; Kosińska, W.; Osmialowski, B.; Gawinecki, R. *Chem. Rev.* **2005**, 105, 3561–3612.
- (7) Osmialowski, B.; Kolehmainen, E.; Kalenius, E.; Behera, B.; Kauppinen, R.; Sievänen, E. *Struct. Chem.* **2011**, 22, 1143–1151.

- (8) Ośmiałowski, B.; Kolehmainen, E.; Dobosz, R.; Gawinecki, R.; Kauppinen, R.; Valkonen, A.; Koivukorpi, J.; Rissanen, K. *J. Phys. Chem. A* **2010**, *114*, 10421–10426.
- (9) Ośmiałowski, B.; Kolehmainen, E.; Gawinecki, R.; Dobosz, R.; Kauppinen, R. *J. Phys. Chem. A* **2010**, *114*, 12881–12887.
- (10) Ośmiałowski, B.; Kolehmainen, E.; Gawinecki, R.; Kauppinen, R.; Koivukorpi, J.; Valkonen, A. *Struct. Chem.* **2010**, *21*, 1061–1067.
- (11) Ośmiałowski, B.; Kolehmainen, E.; Kauppinen, R.; Kowalska, M. *Supramol. Chem.* **2011**, *23*, 579–586.
- (12) Ośmiałowski, B.; Dobosz, R. *J. Mol. Model.* **2011**, *17*, 2491–2500.
- (13) Jorgensen, W. L.; Pranata, J. *J. Am. Chem. Soc.* **1990**, *112*, 2008–2010.
- (14) Pranata, J.; Wierschke, S. G.; Jorgensen, W. L. *J. Am. Chem. Soc.* **1991**, *113*, 2810–2819.
- (15) Gallant, M.; Phan, V. M. T.; Wuest, J. D. *J. Am. Chem. Soc.* **1991**, *113*, 721–723.
- (16) Szyz, Ł.; Guo, J.; Yang, M.; Dreyer, J.; Tolstoy, P. M.; Nibbering, E. T. J.; Czarnik-Matusewicz, B.; Elsaesser, T.; Limbach, H.-H. *J. Phys. Chem. A* **2010**, *114*, 7749–7760.
- (17) Aakeröy, C. B.; Rajbanshi, A.; Li, Z. J.; Desper, J. *CrystEngComm* **2010**, *12*, 4231–4239.
- (18) Fathalla, M.; Lawrence, C. M.; Zhang, N.; Sessler, J. L.; Jayawickramarajah, J. *Chem. Soc. Rev.* **2009**, *38*, 1608–1620.
- (19) Brunsveld, L.; Folmer, B. J. B.; Meijer, E. W.; Sijbesma, R. P. *Chem. Rev.* **2001**, *101*, 4071–4098.
- (20) Burrows, A. D. In *Supramolecular assembly via hydrogen bonds*; Mingos, D. M. P., Ed.; Springer: Berlin/Heidelberg, 2004; pp 55–96.
- (21) Sijbesma, R. P.; Meijer, E. W. *Chem. Commun.* **2003**, 5–16.
- (22) Taubitz, J.; Lüning, U. *Aust. J. Chem.* **2009**, *62*, 1550–1555.
- (23) Lüning, U.; Köhl, C.; Uphoff, A. *Eur. J. Org. Chem.* **2002**, 2002, 4063–4070.
- (24) Taubitz, J.; Lüning, U. *Eur. J. Org. Chem.* **2008**, 2008, 5922–5927.
- (25) Gawinecki, R.; Ośmiałowski, B.; Kolehmainen, E.; Kauppinen, R. *J. Phys. Org. Chem.* **2001**, *14*, 201–204.
- (26) Corbin, P. S.; Zimmerman, S. C.; Thiessen, P. A.; Hawryluk, N. A.; Murray, T. J. *J. Am. Chem. Soc.* **2001**, *123*, 10475–10488.
- (27) Chien, C.-H.; Leung, M.-k.; Su, J.-K.; Li, G.-H.; Liu, Y.-H.; Wang, Y. *J. Org. Chem.* **2004**, *69*, 1866–1871.
- (28) Jordan, L. M.; Boyle, P. D.; Sargent, A. L.; Allen, W. E. *J. Org. Chem.* **2010**, *75*, 8450–8456.
- (29) Bolte, M.; Kuhl, C.; Lüning, U. *Acta Cryst. E* **2001**, *57*, o502–o504.
- (30) Hisamatsu, Y.; Shirai, N.; Ikeda, S.-I.; Odashima, K. *Org. Lett.* **2010**, *12*, 1776–1779.
- (31) Gooch, A.; McGhee, A. M.; Pellizzaro, M. L.; Lindsay, C. I.; Wilson, A. J. *Org. Lett.* **2011**, *13*, 240–243.
- (32) Corbin, P. S.; Zimmerman, S. C. *J. Am. Chem. Soc.* **2000**, *122*, 3779–3780.
- (33) Fu, A.; Li, H.; Du, D.; Zhou, Z. *J. Phys. Chem. A* **2005**, *109*, 1469–1477.
- (34) Yang, M.; Szyz, Ł.; Dreyer, J.; Nibbering, E. T. J.; Elsaesser, T. *J. Phys. Chem. A* **2010**, *114*, 12195–12201.
- (35) Sagvolden, E.; Furche, F. *J. Phys. Chem. A* **2010**, *114*, 6897–6903.
- (36) Müller, A.; Losada, M.; Leutwyler, S. *J. Phys. Chem. A* **2004**, *108*, 157–165.
- (37) Borowiak, T.; Wolska, I.; Korzański, A.; Milius, W.; Schnick, W.; Antkowiak, W. Z. *Naturforsch., B: Chem. Sci.* **2000**, *55B*, 5–11.
- (38) Clarke, M. L.; Fuentes, J. A. *Angew. Chem., Int. Ed.* **2007**, *46*, 930–933.
- (39) Bolz, I.; Spange, S. *Chem.—Eur. J.* **2008**, *14*, 9338–9346.
- (40) Ośmiałowski, B.; Kolehmainen, E.; Ikonen, S.; Ahonen, K.; Löfman, M. *J. Mol. Struct.* **2011**, *1006*, 678–683.
- (41) Sartorius, J.; Schneider, H.-J. *Chem.—Eur. J.* **1996**, *2*, 1446–1452.
- (42) Zimmerman, S. C.; Murray, T. J. *Phil. Trans. R. Soc. Lond., A* **1993**, *345*, 49–56.
- (43) Zimmerman, S. C.; Kwan, W.-S. *Angew. Chem., Int. Ed.* **1995**, *34*, 2404–2406.
- (44) Hupp, T.; Sturm, C.; Basilio Janke, E. M.; Cabre, M. P.; Weisz, K.; Engels, B. *J. Phys. Chem. A* **2005**, *109*, 1703–1712.
- (45) Zafar, A.; Geib, S. J.; Hamuro, Y.; Carr, A. J.; Hamilton, A. D. *Tetrahedron* **2000**, *56*, 8419–8427.
- (46) Wolinski, K.; Hinton, J. F.; Pulay, P. *J. Am. Chem. Soc.* **1990**, *112*, 8251–8260.
- (47) Cheeseman, J. R.; Trucks, G. W.; Keith, T. A.; Frisch, M. J. *J. Chem. Phys.* **1996**, *104*, 5497–5509.
- (48) Bader, R. F. W. *Atoms in Molecules: A Quantum Theory*; Oxford University Press: New York, 1990.
- (49) Popelier, L. A. *Atoms in molecule. An introduction*; Pearson Education: London, 2000.
- (50) Espinosa, E.; Molins, E.; Lecomte, C. *Chem. Phys. Lett.* **1998**, *285*, 170–173.
- (51) Espinosa, E.; Souhassou, M.; Lachekar, H.; Lecomte, C. *Acta Crystallogr.* **1999**, *B55*, 563–572.
- (52) Ośmiałowski, B.; Krygowski, T. M.; Dominikowska, J.; Palusiak, M. *New J. Chem.* **2011**, *35*, 1433–1439.
- (53) Ośmiałowski, B. *J. Mol. Struct. THEOCHEM* **2009**, *908*, 92–101.
- (54) Etter, M. C. *Acc. Chem. Res.* **1990**, *23*, 120–126.
- (55) Gueffier, A.; Viols, H.; Blache, Y.; Chapat, J. P.; Chavignon, O.; Teulade, J. C.; Fauvelle, F.; Grassy, G.; Dauphin, G. *J. Heterocycl. Chem.* **1997**, *34*, 765–771.
- (56) Chen, J.-S.; Rosenberger, F. *Tetrahedron Lett.* **1990**, *31*, 3975–3978.
- (57) Benesi, H.; Hildebrand, J. *J. Am. Chem. Soc.* **1949**, *71*, 2703–2707.
- (58) Frisch, M. J.; Trucks, G. W.; Schlegel, H. B.; Scuseria, G. E.; Robb, M. A.; Cheeseman, J. R.; Montgomery, J., J. A.; Vreven, T.; Kudin, K. N.; Burant, J. C.; Millam, J. M.; Iyengar, S. S.; Tomasi, J.; Barone, V.; Mennucci, B.; Cossi, M.; Scalmani, G.; Rega, N.; Petersson, G. A.; Nakatsuji, H.; Hada, M.; Ehara, M.; Toyota, K.; Fukuda, R.; Hasegawa, J.; Ishida, M.; Nakajima, T.; Honda, Y.; Kitao, O.; Nakai, H.; Klene, M.; Li, X.; Knox, J. E.; Hratchian, H. P.; Cross, J. B.; Adamo, C.; Jaramillo, J.; Gomperts, R.; Stratmann, R. E.; Yazyev, O.; Austin, A. J.; Cammi, R.; Pomelli, C.; Ochterski, J. W.; Ayala, P. Y.; Morokuma, K.; Voth, G. A.; Salvador, P.; Dannenberg, J. J.; Zakrzewski, V. G.; Dapprich, S.; Daniels, A. D.; Strain, M. C.; Farkas, O.; Malick, D. K.; Rabuck, A. D.; Raghavachari, K.; Foresman, J. B.; Ortiz, J. V.; Cui, Q.; Baboul, A. G.; Clifford, S.; Cioslowski, J.; Stefanov, B. B.; Liu, G.; Liashenko, A.; Piskorz, P.; Komaromi, I.; Martin, R. L.; Fox, D. J.; Keith, T.; Al-Laham, M. A.; Peng, C. Y.; Nanayakkara, A.; Challacombe, M.; Gill, P. M. W.; Johnson, B.; Chen, W.; Wong, M. W.; Gonzalez, C.; Pople, J. A. *Gaussian 03*, Revision E.01; Gaussian, Inc.: Pittsburgh PA, 2004.
- (59) Zhao, Y.; Schultz, N. E.; Truhlar, D. G. *J. Chem. Phys.* **2005**, *123*, 161103–161104.
- (60) Zhao, Y.; Truhlar, D. G. *J. Chem. Theory Comput.* **2006**, 1009–1018.
- (61) Zhao, Y.; Truhlar, D. G. *J. Chem. Theory Comput.* **2008**, *4*, 1849–1868.
- (62) Zhao, Y.; Truhlar, D. G. *Theor. Chem. Acc.* **2008**, *120*, 215–241.
- (63) Ditchfield, R.; Hehre, W. J.; Pople, J. A. *J. Chem. Phys.* **1971**, *54*, 724–728.
- (64) Hehre, W. J.; Ditchfield, R.; Pople, J. A. *J. Chem. Phys.* **1972**, *56*, 2257–2261.
- (65) Tomasi, J.; Cammi, R.; Mennucci, B.; Cappelli, C.; Corni, S. *Phys. Chem. Chem. Phys.* **2002**, *4*, 5697–5712.
- (66) Boys, S. F.; Bernardi, F. *Mol. Phys.* **1970**, *19*, 553–566.
- (67) Simon, S.; Duran, M.; Dannenberg, J. J. *J. Chem. Phys.* **1996**, *105*, 11024–11031.
- (68) Peng, C.; Schlegel, H. B. *Isr. J. Chem.* **1993**, *33*, 449–454.
- (69) Biegler-König, F.; Schönbohm, J.; Bayles, D. *J. Comput. Chem.* **2001**, *22*, 545–559.